Chapter 1

Introduction and literature review

1.1 Motivation of thesis

The structural flexibility associated with the oxide-based perovskite (ABO_3) system allows them to host various fascinating properties such as ferroelectricity, ferromagnetism, ferroelasticity, etc. [15, 16, 17, 18]. Out of these, ferroelectrics are well known for their diverse functionality, which makes them suitable candidates for various devices, *viz.,* sensors, actuators, transducers, energy harvesters, memory devices, etc. [19, 20, 21, 22, 23, 24, 25, 26]. The huge market of ferroelectric devices is nowadays dominated by the lead-based ceramic system $Pb(Zr,Ti)O_3$ (solid solution of $PbTiO_3$ with $PbZrO_3$) [27, 28, 29, 30]. However, due to the toxic and hazardous nature of lead-based materials, necessary measures have been taken by various countries of the World to restrict the content of lead in various electronic products. For instance, European Union issued a decree in 2002 to restrict the use of lead-based materials in various commercial products [31, 32]. Thus the increase in awareness about environmental contamination by the use of lead-based materials has stirred a wave of research in lead-free eco-friendly materials [6, 33, 34, 35]. The high physical properties of the lead-based ceramics are achieved via compositional engineering, *i.e.,* by optimizing the designed system (solid solution) in the proximity of the morphotropic phase boundary

(coexistence of the ferroelectric phases with weak temperature dependence) or by inducing a relaxor behaviour in the material [36]. At the morphotropic phase boundary composition, the free energy barrier between the coexisting phases gets minimized, facilitating an easy polarization rotation phenomenon resulting into high physical responses [37, 38]. On the other hand, the relaxor ferroelectricity originates due to polar nano-regions (driven by the locally off-centered atoms) present at the microscopic level in the macroscopic cubic matrix [39, 40, 41]. Although no such lead-free ceramics exhibiting a versatile performance better than the lead-based materials have been discovered yet, however, various 'A' and 'B' site-modified $BaTiO_3$-based solid solutions have shown the potential to exhibit the physical properties comparable to that of lead-based ceramic system. The potential to deliver the excellent physical properties by 'A' and 'B' site-modified $BaTiO_3$-based lead-free solid solutions is linked with the presence of (a) morphotropic phase boundary (nearly vertical phase boundary on the composition-temperature plane), (b) polymorphic phase boundaries (having curvature in the phase boundary), and (c) relaxor ferroelectric behaviour in their phase diagrams [9, 11, 13, 42, 43, 43, 44, 45, 45, 46, 47, 48]. Thus the manipulation in the atomic ordering (both at long and short-range levels) plays a crucial role in the determination of various physical properties of the fabricated solid solutions. Therefore, owing to the idea of relaxor ferroelectrics driven by short-range ordering (polar nano-regions), we have developed a lead-free eco-friendly 'A' and 'B' site-modified $BaTiO_3$-based ceramic systems, *viz.,* $(Ba_{1-x}Ca_x)(Sn_{0.11}Zr_{0.05}Ti_{0.84})O_3$; BCSZT$x$ $(0 \leq x \leq 0.20)$, which exhibits relaxor nature and thus the ferroelectricity in an average cubic phase. Our analysis has shown a correlated local off-centering of atoms corresponding to A(Ca^{2+}) and B(Ti^{4+}) sites in BCSZTx ceramics which is analogous to the cooperative off-centering of Pb^{2+} and Ti^{4+} cations observed in the tetragonal symmetry of $PbTiO_3$. However, the off-centering of the A(Ca^{2+}) site cation in BCSZTx ceramics is attributed to the smaller ionic radii of Ca^{2+} cations than Ba^{2+}, in contrast to the covalent nature of Pb-O bond held responsible

for the off-centering of Pb^{2+} cations in $PbTiO_3$ [7, 49]. Further, being a relaxor ferroelectric, we have explored the presence of an electrostrictive like effect corresponding to composition Ca(x) = 0.15. Subsequently, in order to have an insight into the role of inter-ferroelectric phase boundary (coexistence of long-range ferroelectrically ordered atomic arrangements having different space groups), with the ferroelectric phases driven by the component(s) freezing of three-dimensional polar (Γ_4^-) phonon mode corresponding to the center of cubic Brillouin zone, we have developed another eco-friendly solid solution $(Ba_{0.92}Ca_{0.08})(Zr_{0.05}Ti_{0.95\text{-}x}Sn_x)O_3$; BCZTSn$x$ $(0 \leq x \leq 0.10)$. Our analysis has revealed a significant impact of the amplitude of frozen phonon modes in tuning the ferroelectric properties. Further, for the higher 'Sn' content of BCZTSnx $(0.125 \leq x \leq 0.25)$, a relaxor ferroelectric behaviour has been observed, which is linked with the random stress field generated due to the presence of different ionic radii cations corresponding to 'A' and 'B' site of the perovskite structure. Thus, altogether this thesis work focuses on the impact of long and short-range atomic ordering on the ferroelectric properties of perovskite-based lead-free functional materials.

1.2 Ferroelectricity

The word ferroelectric was first proposed by Erwin Schrodinger in 1912, analogous to ferromagnetism, after predicting that certain liquids can be spontaneously polarized as they solidify [50, 51, 52]. However, ferroelectricity was first observed by Valasek in 1921 for Rochelle salt ($KNaC_4H_4O_6.4H_2O$; potassium sodium tartrate tetrahydrate). When Valasek subjected the sample of this material to the electric field, he found some unusual behaviour in the polarization (P) of the material [51, 53]. He observed that with the increase in the electric field, the polarization increases following an S shape path, and with the lowering of the electric field, polarization follows a similar shape path but with relatively high values of polarization, indicating that the value of polarization depends on the rising or falling

nature of the applied electric field. Thus the material was showing hysteresis [51]. Also, Valasek performed the measurements for the temperature range -20 to +20 ^{0}C and found that the material exhibits a polar nature. Further, by applying a suitable electric field, the direction of the polar axis can be switched. This characteristic behaviour is referred to as ferroelectricity nowadays [52].

1.2.1 Definition, characteristics, and other related phenomena

Ferroelectricity refers to the phenomenon where the materials possess a spontaneous polarization that can be switched on the application of a suitable electric field [21, 54]. Generally, ferroelectric materials exhibit a structural phase transition from a ferroelectric to non-ferroelectric (paraelectric) phase at high temperatures, with the symmetry of the ferroelectric (FE) phase being lower than that of the paraelectric (PE) phase. The temperature at which the FE to PE phase transition takes place is referred to as the Curie temperature (T_c) [55]. In ferroelectric materials, the dielectric permittivity curve follows the Curie-Weiss law above the Curie temperature, which is described as [19, 21]

$$\varepsilon^{'} = \frac{C}{(T - T_{\mathrm{cw}})} \tag{1.1}$$

Here, C represents the Curie constant, while T_{cw} ($T_{cw} \leq T_c$) corresponds to the Curie-Weiss temperature. In addition, as mentioned above, the most important characteristic of a ferroelectric material is polarization *vs.* electric field behaviour, which is driven by the domain wall switching [19, 55]. When the field increases, the polarization of the domains having the unfavourable direction of polarization shows a propensity to switch towards the direction of the applied electric field. When the field is small, the polarization varies linearly with the applied alternating electric field. Fur-

ther, as the field increases, the polarization of the domains having the unfavourable direction of polarization starts switching along the direction of the applied electric field. In this region, the polarization behaviour is non-linear, but as all the domains are aligned, it again becomes linear. Likewise, when the electric field starts decreasing, the domains begin to switch back in the field's direction, and at zero field, a non-zero value of polarization is observed, which is termed as remnant polarization (P_r). In order to make the polarization zero, the applied field is reversed, and the field at which the polarization becomes zero is called the coercive field (E_c). When the field is further increased in the reverse direction, a point is reached having the saturation of polarization. On completing the cycle, a hysteresis loop is obtained as shown in Fig. 1.1 [19, 55].

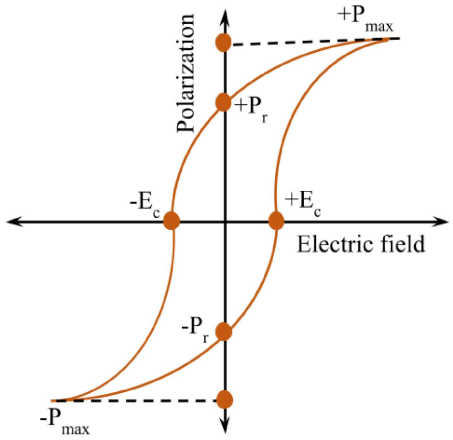

Fig. 1.1 Polarization *vs.* electric field (PE) hysteresis loop for a typical ferroelectric, having the remnant polarization (P_r) and coercive field (E_c).

In general, ferroelectricity is described with two other phenomena, *viz.,* pyroelectricity and piezoelectricity. Briefly, pyroelectricity is identified as the effect where the crystal lacks inversion symmetry and has a unique symmetry axis that exhibits the separation between the positive and negative charges when the temperature changes [52, 56, 57]. If this material is placed between the two electrodes (a dielectric within a capacitor), the capacitor plates keep on charging until the charges present on the surface of the pyroelectric materials gets neutralised [58]. If the pyroelectric material is heated, then the dipoles start loosing their alignment leading to a flow of current in the external circuit. On the other hand, the spontaneous polarization increases on cooling as the dipoles regain their orientations, which in turn reverses the direction of the current [58]. The expression for

pyroelectric current (i_{p}) is given by the following equation [59],

$$i_{\mathrm{p}} = pA\frac{dT}{dt} \tag{1.2}$$

Here, A represents the surface area of the material, $\frac{dT}{dt}$ defines the rate of change of temperature, and p is the pyroelectric coefficient. The coefficient p of an unclamped material under constant stress (σ), and electric field (E) is given by

$$p^{\sigma,\mathrm{E}} = \left(\frac{dP_{\mathrm{s}}}{dT}\right)_{\sigma,\mathrm{E}} \tag{1.3}$$

where P_{s} represents the spontaneous polarization. This ability of change in temperature to produce the pyroelectric current is widely used in the field of infrared and terahertz detectors and in energy harvesting [56, 59].

On the other hand, piezoelectricity refers to the phenomenon where some materials exhibit a change in polarization when subjected to mechanical stress because of having a crystal structure that lacks the center of inversion symmetry [60, 61]. This means that on the subjection of mechanical stress, piezoelectric material deforms, and the generation of electric charges takes place. The process of generation of electric charge via mechanical stress is the direct piezoelectric effect. In contrast, when a piezoelectric material is subjected to an external electric field, then the material gets mechanically deformed, and this phenomenon is referred to as the converse piezoelectric effect (see Fig. 1.2) [62]. Piezoelectricity is generally described by the piezoelectric coefficient (d), which is defined as the ratio of charge per unit area (polarization) and applied stress or by the ratio of strain to the electric field [20].

$$P = \frac{Q}{A} = dX \tag{1.4}$$

$$x = dE \tag{1.5}$$

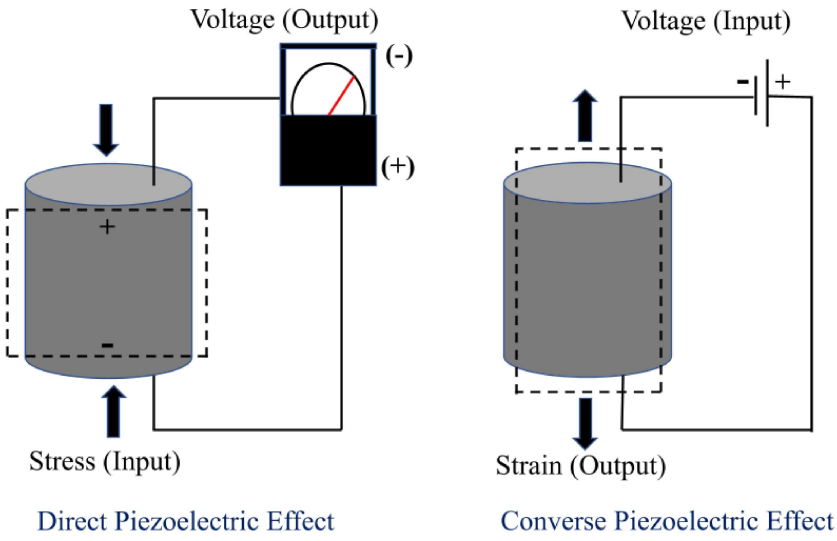

Fig. 1.2 Representation of direct and converse piezoelectric effect.

where Q is the charge, P represents polarization, A is the area, X is the mechanical stress, x represents strain, and E is the applied electric field.

All these phenomena, *viz.,* ferroelectricity, pyroelectricity, and piezoelectricity are closely related to the crystallographic structure of the materials. There are seven crystal systems (cubic, tetragonal, hexagonal, rhombohedral, orthorhombic, monoclinic, and triclinic) which are classified into 32 point groups [20]. Out of these, 21 point groups (432, $\bar{4}3m$, 23, 422, $\bar{4}2m$, $4mm$, $\bar{4}$, 4, $\bar{6}m2$, $6mm$, 622, $\bar{6}$, 6, 32, $3m$, 3, 222, $mm2$, m, 2, and 1) are non-centrosymmetric. These point groups exhibit piezoelectricity, with the exception of point group 432, which does not exhibits piezoelectricity because the symmetry operation in the polarization direction cancels the polarization. On the other hand rest of the 11 point groups ($m3m$, $m3$, $4/mmm$, $4/m$, $6/mmm$, $6/m$, $\bar{3}m$, $\bar{3}$, mmm, $2/m$, and $\bar{1}$) are classified as centrosymmetric ones [20]. Further, out of the 20 piezoelectric point groups, there are ten-point groups (6, $6mm$, 3, $3m$, 4, $4mm$, $mm2$, 2, m, and 1) which are polar in nature and exhibit pyroelectricity [20]. Out of these ten point groups, those which exhibit a polarization reversal when an external electric field is applied are called ferroelectrics [20, 63]. Hence ferroelectric materials are both pyroelectric and piezoelectric

[6]. Therefore, ferroelectrics have remained a subject of investigation for researchers after its discovery for both scientific as well as technological application purposes. In the class of ferroelectric materials, perovskite-based ferroelectrics have been recognized to be extremely important from fundamental science as well as technological points of view.

1.3 Perovskite structure

Perovskites are characterized as the class of compounds with structures resembling that of the mineral perovskite, $CaTiO_3$, and have been considered to be derived from a parent structure with the general formula ABO_3 (see Fig. 1.3) [64, 65]. It was discovered by the mineralogist Gustav Rose in mineral deposits of the Ural Mountains around 1839 and named after the Russian mineralogist Count Lev Alekseyevich von Perovski. They have been extensively studied due to their various excellent properties hosting a wide variety, *viz.,* ferroelectric, dielectric, piezoelectric, superconductivity, optical properties, multiferroic properties, magnetic ordering, etc. This wide variety of properties hosted by perovskite lies in their structural flexibility, which ranges from simple cubic (ideal perovskite) to various other distorted complex phases [66, 67].

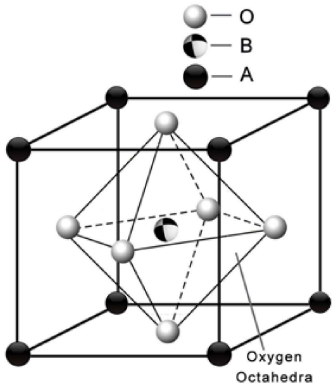

Fig. 1.3 The representation of the unit cell of an ideal cubic perovskite (ABO_3) structure.

1.3.1 Tolerance factor and structural stability

The ideal perovskite (ABO_3) structure is rigid from a crystallographic point of view, having a centrosymmetric cubic ($Pm\bar{3}m$) phase with fixed atomic positional coordinates [68, 69, 70]. In an ideal case, the 'A' site atoms are located at the corners of the cube, and

oxygens atoms reside at the faces of the cube forming an [BO_6] octahedral cage whose center is occupied by 'B' site cations (see Fig. 1.3) [65, 71, 72, 73]. The structures of oxide-based perovskites are generally characterized by using the tolerance factor (t) given by the following equation [74, 75],

$$t = \frac{(R_A + R_O)}{\sqrt{2}(R_B + R_O)}, \tag{1.6}$$

where R_A and R_B correspond to the ionic radii of the A (XII coordination state) and B (VI coordination state) site cations, respectively, and R_O represents the ionic radii of the oxygen ions [74]. Here, t acts as a structural stability indicator of the various perovskite (ABO_3) based materials [74]. For example, $SrTiO_3$ is an ideal perovskite with the value of tolerance factor t = 1 [65], as deduced below. If 'a' represents the sides of the cube, then along <110> direction, from Fig. 1.3,

$$\sqrt{2}a = 2R_A + 2R_O$$

$$a = \frac{2R_A + 2R_O}{\sqrt{2}} \tag{1.7}$$

and, along <100> direction;

$$a = 2R_B + 2R_O \tag{1.8}$$

Equating equations (1.7) and (1.8), we get:

$$\frac{2R_A + 2R_O}{\sqrt{2}} = 2R_B + 2R_O$$

$$\implies 1 = \frac{R_A + R_O}{\sqrt{2}(R_B + R_O)}$$

However, the real perovskites may exhibit the tolerance factor (t<1 or t>1) deviating from t = 1. Generally, the perovskite structure is stable for the range of values 0.78<t<1.05 [76, 77]. Thus based on the variations in tolerance factor from the ideal cubic phase, perovskites show complex crystallographic structures [68, 78]. For the perovskite materials having t<1, the A-O bond is elongated by the larger 'B' site cation, which consequently makes the 'A' site cation to move from their ideal position, accompanied by the rotations of the adjacent oxygen octahedra, and thus bending O-B-O bonds [79, 80, 81]. The widely explored system in this category is calcium titanate ($CaTiO_3$), which exhibits an orthorhombic phase (a distorted perovskite structure) having *Pbnm* space group [80, 82]. On the other hand, perovskites having t>1 have a larger 'A' site cation, which elongates the B-O bond length, consequently leading to the shift of the 'B' site cation from its ideal centrosymmetric position. This, in turn, results in the 'B' site-driven ferroelectricity in the materials, *e.g.,* barium titanate ($BaTiO_3$) [79, 80, 81].

1.3.2 Theories to explain ferroelectricity in perovskites

The ferroelectric materials exhibit a phase transition from high symmetry centrosymmetric phase to a low symmetry non-centrosymmetric phase having spontaneous polarization with the decrease in temperature. This phase transition is described by various proposed theories. One of the theories used to describe the paraelectric to ferroelectric phase transition is the soft mode theory. According to the soft mode theory, the frequency of a transverse optical (TO) phonon mode belonging to the zone center of the high symmetry cubic Brillouin zone drops to zero at the transition point and subsequently evolves in the ferroelectric phase, which leads to the displacement of the ions from their high symmetry centrosymmetric positions [52, 83]. The other theory used to explain ferroelectricity is based on the order-disorder approach. According to order-disorder model, the high-temperature phase exhibits a disordered nature characterized by the presence of local distortions consistent with the

constraints of the low-temperature ferroelectric phase. Further, the resultant of these local distortions change as a function of temperature, and finally, at low temperatures, these local distortions become completely ordered due to cooperative dipole interactions, leading to a completely ordered ferroelectric phase [52, 84]. The ferroelectric instability is also explained by the balance between the bonding considerations that try to stabilize the ferroelectric phase and the short-range repulsions that favour the paraelectric (non-ferroelectric) phase [16, 85]. In the perovskite materials, exhibiting only the ionic nature of bonding, the most favourable structure is the centrosymmetric, *i.e.,* non-ferroelectric [86]. The reason behind the stabilization of the centrosymmetric phase is the short-range repulsive force acting between the adjacent ions [86]. On the other hand, ferroelectrically distorted structures result due to hybridization between the transition metal cation and the surrounding anions. This results in an off-centered displacement of the small cation from its centrosymmetric position [9, 87]. For example, ferroelectricity in lead titanate ($PbTiO_3$) and barium titanate ($BaTiO_3$), is governed by the hybridization between the Ti($3d$) and O($2p$) states [16]. However, the essential requirement of this mechanism is that the d orbital of the transition metal cation be formally unoccupied [88]. Another mechanism of ferroelectricity occurs around the cations that possess an ns^2 type valence electrons, such as Pb^{2+}, which contains $6s^2$ lone pair electrons (electron pairs which don't involve in the formation of chemical bonds directly) in the outermost shell [16, 89]. In $PbTiO_3$, the sp hybridization taking place between the lead and oxygen ions reduces short-range repulsion, resulting in large polar distortions, which is referred to as lone-pair driven ferroelectricity in the literature [16, 90, 91]. In general, the lone pair repulsive forces impact the spatial distribution of bonding electron pairs when applied to other bonding schemes. Therefore an asymmetric local coordination environment gets created, which consequently leads to a non-centrosymmetric structure having enhanced physical properties, *viz.,* ferroelectricity, piezoelectricity, etc. [88, 90].

1.3.3 Role of soft phonon modes in structural phase transformation of perovskites

As a well-established fact, perovskites (ABO_3) are known to undergo various structural phase transitions when subjected to external stimuli, *e.g.,* temperature, pressure, composition, etc. [68, 92]. The various structural distortions in perovskites are associated with the different irreducible representations (irreps) linked with the soft phonon modes corresponding to the high-symmetry parent space group [93]. For example, when the 'A' site cations present in the dodecahedra are small in size, then the tilting of BO_6 octahedra takes place in order to reduce the size of the available space around 'A' site cations [76]. The tilting of the adjacent octahedra can happen along any-one or more symmetry axes and can be of the same or different sign with equal or unequal magnitudes. The tilting of the octahedra is characterized by two different ways, *viz.,* in-phase rotation of the octahedra and out-of-phase rotation of the octahedra. The in-phase and out-of-phase rotations are associated with the M and R points of the cubic Brillouin zone (see Fig. 1.4) and are described by the respective irreps, namely M_3^+ and R_4^+ [69, 92, 93]. Further, the octahedral distortions are caused by a change in the length of the B-O bond and deviation of the O-B-O angles from 90^o or 180^o [94, 95, 96]. Furthermore, the structural distortions driven by the off-centering of the 'B' site cation are described by the movement of the associated atom from its centrosymmetric position in the available octahedral space and is governed by the instability associated with the Γ point of the cubic Brillouin zone (see Fig. 1.4) [69, 93, 97]. The structural phase transitions, which are driven by the condensation of the soft phonon mode belonging to the

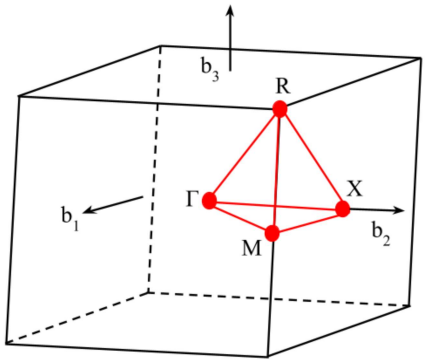

Fig. 1.4 The representation of different points in the Brillouin zone of the cubic lattice.

zone center, are termed as ferrodistortive [21]. However, if the associated phonon mode is polar in nature (related irrep Γ_4^-), then its condensation results in a long-range polar ordering in the material known as 'ferroelectricity' [69]. Although most of the ferroelectric materials are ferrodistortive but sometimes it may not be so. Sometimes, the mode condensation occurs at the point(s) other than the zone center, and the phase transitions driven by such mode condensation are referred to as antiferrodistortive. Further, when a coupling between the modes exists, it is not necessary that the ferroelectric phase transition is driven by the instability associated with the zone center polar mode. Sometimes, the ferroelectric polarization in the material results in an indirect fashion via the coupling of zone center phonon mode with an antiferrodistortive mode acting as a leading order parameter [21]. Such phase transitions are referred to as intrinsically antiferrodistortive but extrinsically ferroelectric [21]. Therefore, in this scenario, antiferrodistortive mode acts as a primary order parameter, whereas spontaneous polarization acts as a secondary order parameter [21]. The next section describes the phase transition behaviour of the first ever discovered perovskite-based ferroelectric barium titanate.

1.3.4 Barium titanate: The first ferroelectric perovskite

The ferroelectricity in the oxide-based perovskite materials was first discovered in $BaTiO_3$ by Wul and Goldman around 1945-1946 [98]. In the series of versatile fundamental ferroelectric materials, barium titanate ($BaTiO_3$), along with another key material, $PbTiO_3$, has received tremendous attention worldwide for various scientific and technological applications [6]. A comparative study of both these ceramics shows that the $PbTiO_3$ exhibits a stronger ferroelectric character than the $BaTiO_3$ [16, 88]. However, nowadays, $PbTiO_3$, as well as solid solutions of $PbTiO_3$ with $PbZrO_3$, $Pb(Mg_{1/3}Nb_{2/3})O_3$, and $Pb(Zn_{1/3}Nb_{2/3})O_3$, are being replaced with their lead-free counterparts. In this regard, $BaTiO_3$-based ceramics have emerged as promising candidates to supplant lead-based ceramics from various tech-

nological applications. Therefore, despite of its discovery a long time ago, it remains of great significance for the researchers to investigate, understand and tailor the structural and physical properties of $BaTiO_3$ for device engineering. From crystallographic point

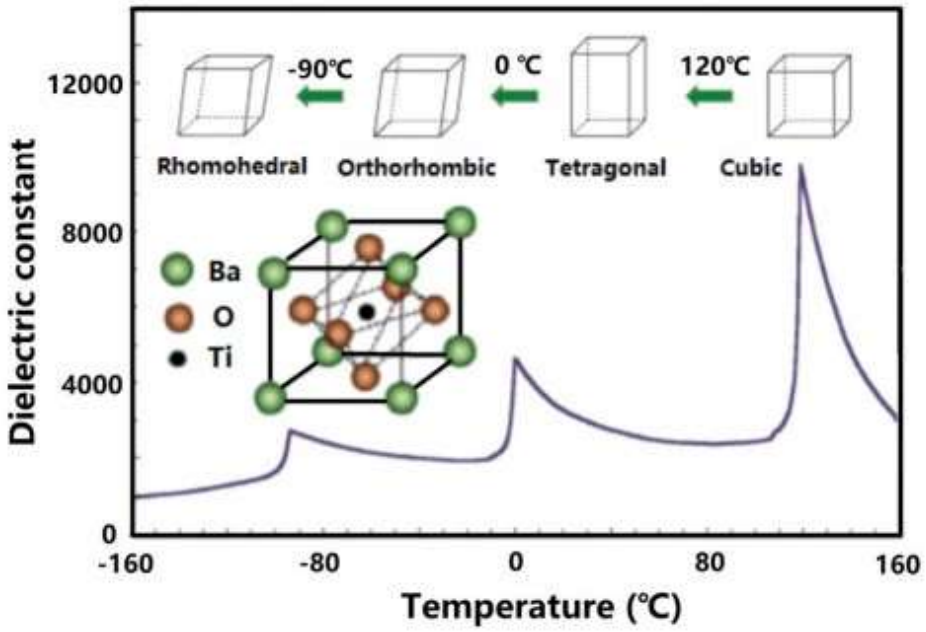

Fig. 1.5 Temperature-dependent variation in the dielectric permittivity of barium titanate [1].

of view, $BaTiO_3$ exhibits a cubic ($Pm\bar{3}m$) phase at high temperatures consistent with the ideal perovskite (ABO_3) structure. With regards to high-temperature cubic cells, Ba^{2+} cations are present at the corners of the cube, O^{2-} ions at the center of faces, resulting in an octahedron, and Ti^{4+} cation locates at the body center of the cube (see Fig. 1.5) [99]. On cooling, $BaTiO_3$ undergoes three successive ferroelectric phase transitions, *viz.,* Cubic (C; $Pm\bar{3}m$) $\xrightarrow{\text{T = 393 K}}$ Tetragonal (T; $P4mm$) $\xrightarrow{\text{T = 273 K}}$ Orthorhombic (O; $Amm2$) $\xrightarrow{\text{T = 183 K}}$ Rhombohedral (R; $R3m$) [99]. These low-symmetry ferroelectric phases *viz.,* $P4mm$, $Amm2$, and $R3m$ are driven by the displacement of Ti^{4+} cations along $\langle 100 \rangle$, $\langle 110 \rangle$, and $\langle 111 \rangle$ directions, respectively [99]. Further, the ferroelectric phase transitions observed in $BaTiO_3$ are generally described by the two models, *viz.,* the displacive model

[100, 101, 102] and the order-disorder model [2, 103]. The mechanism behind these phase transitions, in particular, their order-disorder *vs.* displacive character is still a debatable issue, despite extensive studies. According to the displacive model, which is associated with the soft phonon mode belonging to the Γ point of the cubic Brillouin zone, the above-mentioned phase transitions are driven by the component(s) freezing of the ferroelectric (Γ_4^-) zone center phonon mode [14]. On the other hand, a number of theoretical and experi-

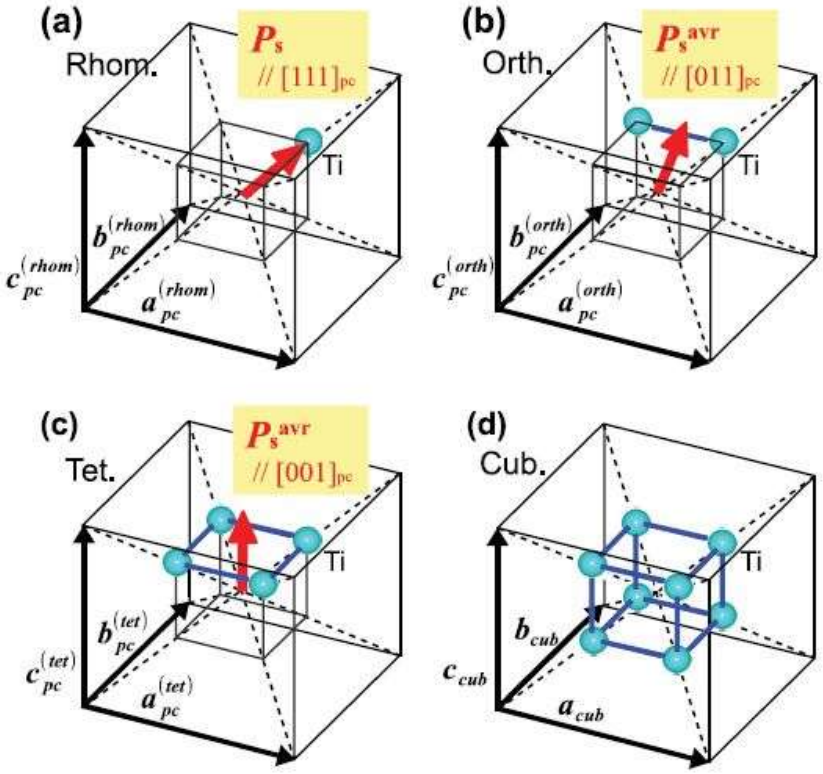

Fig. 1.6 Schematic representation of off-centered Ti atom along ⟨111⟩ directions in (a) rhombohedral, (b) orthorhombic, (c) tetragonal, and (d) cubic phases of $BaTiO_3$ [2].

mental studies, including the eight-sight model [103], nuclear magnetic resonance (NMR) [104, 105], X-ray diffuse scattering [103], electron paramagnetic resonance (EPR) [106], convergent-beam electron diffraction (CBED) [2], extended X-ray absorption fine structure (EXAFS) and X-ray absorption near edge structure (XANES) [107], second harmonic generation [108], first-principles Monte Carlo simulations [109] and Landau-Devonshire

theory [110] have revealed the presence of an order-disorder character. The order-disorder model of phase transitions proposed by Takahasi and Comes *et al.*, considers that the nanometer-sized structures with random off-centered displacements of Ti^{4+} cations along eight equivalent directions exists in the cubic phase (see Fig. 1.6(d)) [103]. On cooling, these randomly off-centered Ti^{4+} cations order along the four adjacent directions resulting into a tetragonal phase with polarization along $\langle 100 \rangle$ directions (see Fig. 1.6(c)). On further cooling, these displacements become ordered along two adjacent directions resulting into orthorhombic phase with polarization along the $\langle 110 \rangle$ direction (see Fig. 1.6(b)), and finally, at very low temperatures, these displacements become ordered along the $\langle 111 \rangle$ direction giving rise to a completely ordered rhombohedral phase (see Fig. 1.6(a)) [103]. It is also observed by some groups that the phase transitions of $BaTiO_3$ involve a mixed order-disorder and displacive characters [104, 111, 112]. Interestingly, $BaTiO_3$ exhibits a high dielectric and ferroelectric polarization, and finds its applications in capacitors, piezoelectric sensors, data-storage devices, etc. [113, 114].

1.4 Idea of phase coexistence in the enhancement of physical properties

Although the properties of $BaTiO_3$ are high, yet it is significantly low in comparison to the lead-based ferroelectric ceramic system, *i.e.,* $Pb(Zr_xTi_{1-x})O_3$. In order to improve the physical properties of $BaTiO_3$, various efforts have been made by different groups via several means, such as chemical substitutions, stress application, particle size tuning, grain size modifications, pressure application, etc. The key feature behind the modification in the properties lies in the tuning of various crystallographic phase(s) and related phase transitions. Owing to its simplicity, chemical substitutions have been identified as the most common approach for modifications in the ferroelectric, dielectric, and piezoelectric

properties. The proper engineering of 'A' and 'B' sites of $BaTiO_3$ through various dopants may lead to the formation of the phase coexistence regions by tuning the ferroelectric to paraelectric and inter-ferroelectric phase transition temperatures. In addition, the large difference in the size and charge of the dopants induces local ordering, which may result into a relaxor ferroelectric phase. The term phase coexistence corresponds to two types of phase boundaries, *viz.,* polymorphic phase boundary (strongly temperature dependent) and morphotropic phase boundary (weakly temperature dependent), and the presence of these boundaries in any ceramic system play a crucial role in the enhancement of the physical properties of the system [6, 37].

1.4.1 Morphotropic and polymorphic phase boundary

The morphotropic phase boundary (MPB) occurs around a particular composition, whereas polymorphic phase boundary (PPB) arises as a function of thermodynamic variables such as temperature, pressure, etc. Out of these, the former one, *i.e.,* MPB, corresponds to the phase boundary that exhibits nearly temperature-independent behaviour represented by a nearly vertical phase boundary on the composition-temperature plane, whereas the latter one, *i.e.,* PPB, corresponds to the curvature in the phase boundary (see Fig. 1.7) [6, 37]. At the morphotropic phase boundary, the ferroelectric and piezoelectric properties become exceptionally high. The enhancement in the properties is attributed to the polarization rotation and (or) polarization extension phenomenon [37, 38], facilitated by the flattening of the free energy profile, and therefore, the transformation takes place from the local minima into a global minima [38, 115, 116]. The polarization rotation phenomenon occurs when the phase transitions are ferroelectric-ferroelectric (FE-FE) type and corresponds to the different directions of polarizations, while the polarization extension occurs when the phase transitions are paraelectric-ferroelectric (PE-FE) in nature [38, 115].

It has been observed that the energy profile at PPB also gets flattened, leading to the polarization rotation phenomenon. Moreover, the polarization extension phenomenon, characterized as field-induced phase transition (reversible in nature), has also been held responsible for the enhanced properties at PPB [37]. However, owing to thermal stability, morphotropic phase boundary compositions are of special technological importance and have been widely explored by various groups in both lead-based as well as lead-free ceramic systems [6, 37, 38]. The idea of the morphotropic phase boundary and its impact on the physical properties (ferroelectric, piezoelectric, etc.) has been very much exploited for the lead-based ceramic systems, *e.g.,* $Pb(Ti_xZr_{1-x})O_3$ [36, 117], $Pb(Mg_{1/3}Nb_{2/3})O_3$-$PbTiO_3$ [118, 119], $Pb(Zn_{1/3}Nb_{2/3})O_3$-$PbTiO_3$ [120, 121], etc. In $Pb(Ti_xZr_{1-x})O_3$ (PZT) ceramics, the morphotropic phase boundary is stable for the composition range $0.48 \leq Ti(x) \leq 0.50$ (see Fig. 1.8) [36, 117]. The MPB in PZT refers to the region, separating the Ti-rich tetragonal ($P4mm$) phase from the Zr-rich rhombohedral ($R3m$) phase, and at $Ti(x) = 0.48$, the MPB exhibits a nearly vertical nature (see Fig. 1.8) [36, 117]. Thus MPB in PZT can be regarded as a phase boundary between the ferroelectric tetragonal and rhombohedral phases [36, 117]. Around MPB, the physical properties (piezoelectric constant, electromechanical coupling coefficients, etc.) attains a maximum value. The reason behind

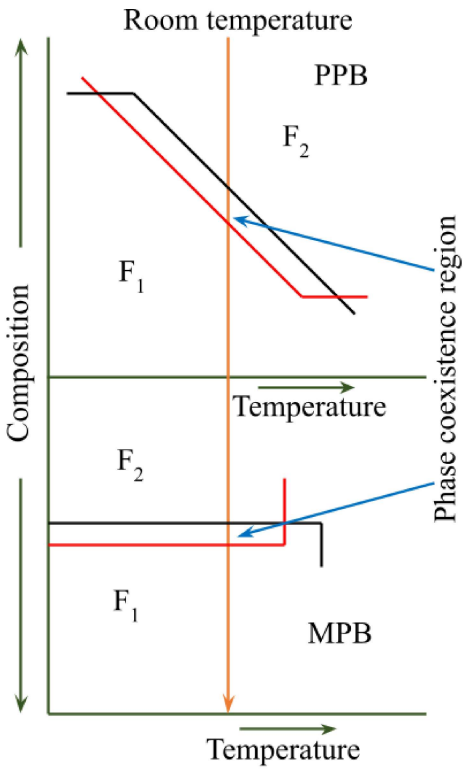

Fig. 1.7 Schematic representation of polymorphic phase boundary (PPB) and morphotropic phase boundary (MPB) existing between two ferroelectric phases, F_1 and F_2.

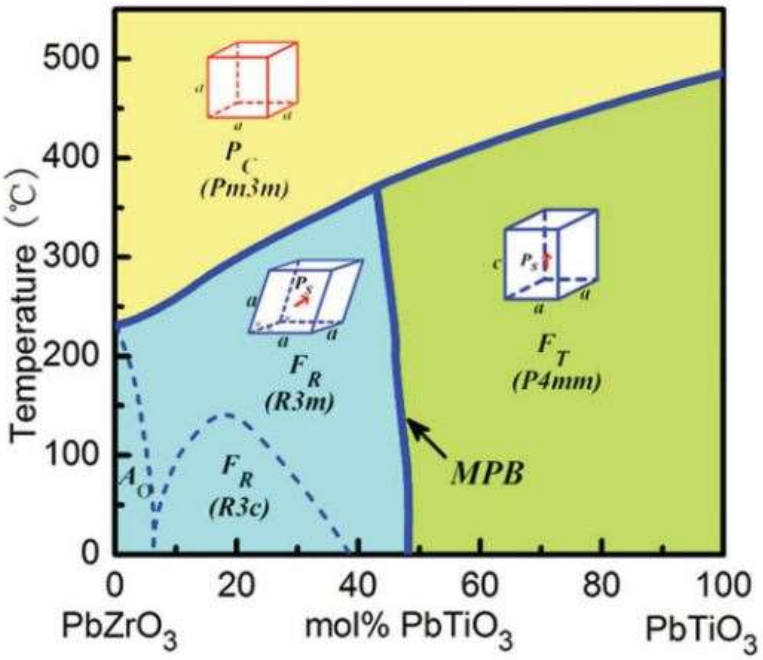

Fig. 1.8 Morphotropic phase boundary in $Pb(Zr,Ti)O_3$ [3].

the maxima in the physical properties has remained a mystery for a long time since the rhombohedral and tetragonal phases are not associated via group subgroup relationship [122]. However, the discovery of a monoclinic phase acts as a bridge between the two phases provides an explanation for the enhanced piezoelectric response via polarization rotation mechanism. Various groups have reported several monoclinic phases in MPB-based systems, *viz.,* M_A, M_B, and M_c, with *Cm*, *Cm*, and *Pm* space groups, respectively [28, 117, 123, 124, 125]. Despite having the same space group, M_A and M_B phases differ via the relationship between the polarization components, *viz.,* P_x, P_y, and P_z, along x, y, and z directions. The M_A and M_B phases are characterized by P_x=P_y<P_z and P_x=P_y>P_z, respectively [29, 123]. Further, the M_A and M_B phases exhibit the cations displacements lying in the {110} planes (see Fig. 1.9) [125]. For the M_A phase, the cation displacements occur between ⟨111⟩ and ⟨100⟩ directions, while for the M_B phase, these displacements lie between ⟨111⟩ and ⟨110⟩ directions [125]. On the other hand, cations displacement

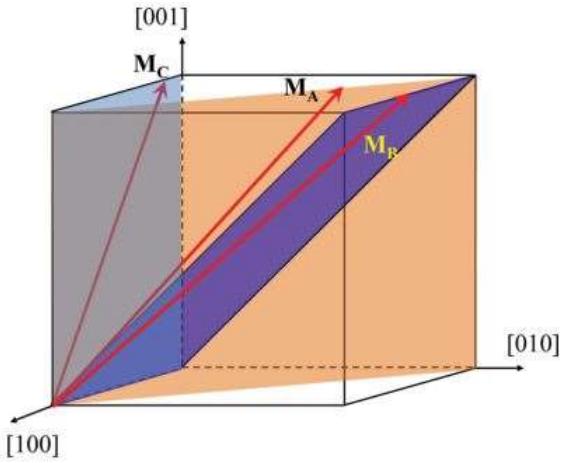

Fig. 1.9 Schematic representation of polar directions in monoclinic M_A, M_B, and M_c phases [4].

corresponding to M_c phase lies on {100} family of planes (see Fig. 1.9) [126]. Thus the unique feature associated with the monoclinic phase is that its polarization vector can lie anywhere in the symmetry plane, in contrast to the specified ⟨100⟩ and ⟨111⟩ directions corresponding to tetragonal and rhombohedral phases [29, 125]. Further, the compositions in the vicinity of the morphotropic phase boundary (having distinct patterns of atomic displacements) exhibits very close free energies corresponding to various phases, indicating a nearly flat energy surface with a minimized energy barrier. Consequently, the local minima become shallow, leading to a global minima, facilitating the easy polarization rotation on the application of electric field [116, 127]. The polarization rotation phenomenon has been considered as one of the most important intrinsic reasons for large piezoelectric properties around MPB in PZT [38, 128]. However, huge piezoresponse is also associated with extrinsic contributions such as domain wall motions, phase boundary motion, etc. [129]. Interestingly, Damjanovic *et al.* observed that at higher temperatures, a triple point (T-R-C) occurs in PZT due to the proximity of C-R, T-R (MPB), and C-T transitions. In addition to the polarization rotation, the polarization extension phenomenon also takes place at the

triple point due to the presence of paraelectric and ferroelectric phases simultaneously [38].

Further, in addition to the above-mentioned MPB-based ferroelectric systems resulting in technologically important physical properties, there is another class of ferroelectrics popularly known as relaxor ferroelectrics has got considerable attention due to its thermally stable and high physical responses.

1.5 Relaxor ferroelectrics

Relaxor ferroelectrics (or relaxors) have remained a very popular topic of research after its discovery by Smolenskii and Agranovskaya in 1959. The unique features associated with relaxors have attained considerable attraction in recent years, and are getting continuous attention owing to the wide variety of industrial applications. Relaxor ferroelectrics possess fascinating electromechanical properties useful for transducers, and nearly temperature-independent high dielectric response suitable for thermally stable dielectric devices. Another underlying reason behind their attraction in the research community lies in their microscopically different behaviour in contrast to macroscopic structure, which plays a crucial role in the determination of exotic physical properties of the relaxors [40, 130, 131].

1.5.1 Definition and characteristics

Relaxors are the materials that are characterized by a broad maxima in the temperature-dependent dielectric permittivity curve, and the temperature corresponding to maxima, *i.e.,* T_m, shifts toward high temperatures on increasing the frequency of the probing field (see Fig. 1.10) [132, 133, 134, 135]. In contrast to normal ferroelectrics, the temperature T_m in relaxors does not correspond to a structural phase transition from paraelectric to a

long-range-ordered ferroelectric phase [135, 136]. Instead, the polarization in relaxors is due to the correlations between the local scale structures, *i.e.,* polar nano-regions (typically 2-10 nm), which plays a key role in the determination of the physical properties of relaxors (see Fig. 1.11) [136, 137]. In contrast to normal ferroelectric materials that exhibit a well-defined Curie temperature (T_c), the relaxors are described by several characteristic temperatures, *viz.,* Burn temperature (T_B) [138], the temperature so-called T^* [139, 140, 141], the frequency-dependent temperature corresponding to the dielectric maxima (T_m) [39], and the Vogel-Fulcher freezing temperature (T_{VF}) [142]. For temperatures higher than T_B, the paraelectric cubic phase of relaxors exhibits similar behaviour as that of the cubic phase of normal ferroelectrics [40]. However, upon cooling, the dynamical polar nano-regions (PNRs) start appearing at T_B, and further lowering of temperature leads to the formation of static atomic displacements at T^*. On further lowering the

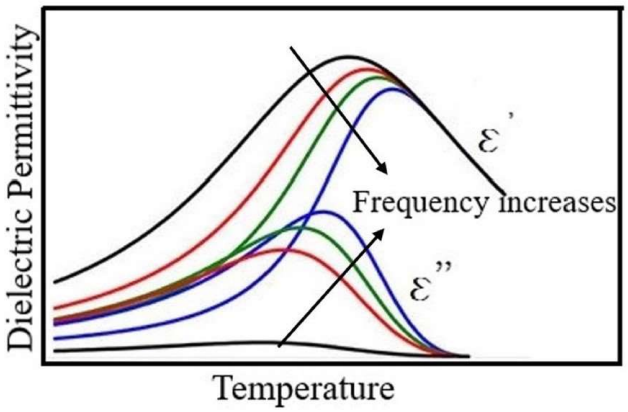

Fig. 1.10 Schematic representation of dielectric permittivity behaviour exhibited by relaxor ferroelectrics [5].

temperatures below T^*, the size of the PNRs increases, and they start impinging on each other, leading to a frequency-dependent temperature corresponding to dielectric maxima, *i.e.,* T_m. On further cooling, the dynamics of PNRs slows down and finally freezes at temperature T_{VF}. Owing to such temperature-dependent dielectric permittivity behaviour, relaxor ferroelectrics do not follow the Curie-Weiss law (see equation (1.1)). In the case of

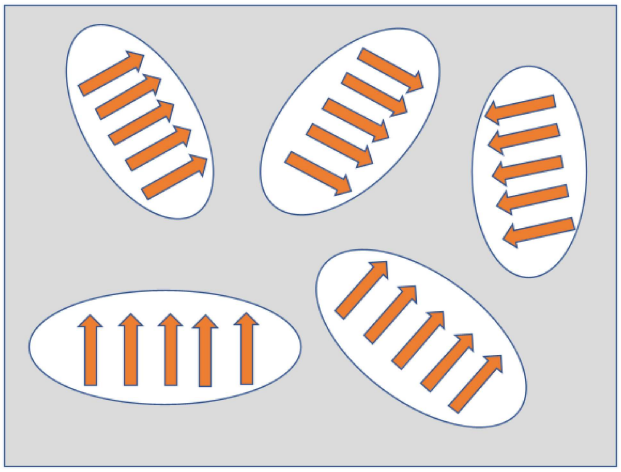

Fig. 1.11 Schematic representation of polar nano-regions in the cubic matrix.

relaxors, this law is applicable only for the temperatures above the Burn temperature, and deviation from Curie-Weiss law starts below the Burn temperature due to the appearance of polar nano-regions [40]. Hence, in order to describe the relaxor ferroelectric behaviour Uchino proposed a modified Curie-Weiss law, which is given as [143],

$$\frac{1}{\varepsilon'} - \frac{1}{\varepsilon'_{\mathrm{m}}} = \frac{(T - T_{\mathrm{m}})^{\gamma}}{C}; T > T_{\mathrm{m}} \tag{1.9}$$

where $\varepsilon'_{\mathrm{m}}$ is the value of dielectric permittivity corresponding to $\mathrm{T_m}$, and γ is called the diffusion exponent whose value lies between $1 \leq \gamma \leq 2$. The limiting values, *i.e.,* $\gamma = 1$, characterizes an ideal ferroelectric, whereas $\gamma = 2$ corresponds to a relaxor ferroelectric [144, 145]. Thus, the polar nano-regions in relaxors are the key feature behind their unique physical properties and dramatically distinct behaviour than the normal ferroelectrics. In relaxors, as far as cooling takes place, the number and size of the PNRs, as well as the interaction between them increases [146]. The decrease in temperature reduces the mobility of the PNRs as the thermal energy is no longer capable of switching the polarization state of PNRs. The freezing of the PNRs starts at slightly higher temperatures than $\mathrm{T_m}$ and finishes at a temperature slightly below $\mathrm{T_m}$ [147]. As mentioned above, the physical

responses (dielectric and ferroelectric, etc.) of the relaxors are highly dependent on the dynamics of the PNRs, interaction between the PNRs, and the response of PNRs as a function of the applied external electric field. When a weak field is applied, the unfrozen regions and the frozen regions having an activation energy of the order of K_BT switches as a function of the externally applied field and therefore contributes in the dielectric response of the material [147]. However, the switching of all these regions can not be done at any excitation frequency, and the number of PNRs that follow the applied external electric field switching decreases with an increase in the frequency [147]. In addition, the response of the relaxors also depends on the relaxation time of such regions. Thus dielectric properties of the relaxor ferroelectric materials are the function of the number of PNRs that can contribute at each temperature and the distribution of the corresponding relaxation time of these PNRs [147]. Moreover, below the freezing temperature, the size of the PNRs and interaction between them becomes so large that the contribution from these regions in dielectric permittivity gets significantly reduced as the applied electric field is unable to switch them and is insufficient to break the strong interactions between the large PNRs [147]. In addition to such an interesting dielectric behaviour, the relaxor ferroelectric materials are characterized by their slim hysteresis loop with a low remnant polarization, in contrast to the normal ferroelectrics having a square shape loop with large remnant polarization [148]. The relaxors exhibit a typical hysteresis loop in the vicinity of the freezing temperature. At high temperatures, the thermal energy in relaxors causes fluctuations between the equivalent polarisation states, and therefore, the dipoles cannot be reoriented by the electric field [147]. However, on decreasing the temperature, the energy barrier between the equivalent polarization states increases, and now the dipoles can be oriented by the electric field, leading to the enhancement in ferroelectric polarization [147]. Due to such interesting phenomena, relaxors are getting continuous attraction from scientific as well as technological point of view. However, despite having great attention

from the scientific community, the understanding of the relaxors is still not very much clear. In order to explain the unique features of relaxor ferroelectrics, different competing models have been proposed.

1.5.2 Some models for relaxor ferroelectrics

The first model to explain the relaxors was proposed by Smolenskii, which is known as the compositional heterogeneity model [149]. According to this model, the cations corresponding to the 'B' sites in Pb(B'B")O_3 [*e.g.,* Pb($Mg_{1/3}Nb_{2/3}$)O_3] are randomly distributed. Such distribution leads to chemically inhomogeneous micro-regions, which causes a spatial fluctuation in the local Curie temperature. On lowering the temperature, local ferroelectric phase transitions take place primarily for those regions (inhomogeneous micro-regions) whose local Curie temperature is high. Consequently, a broad peak in the dielectric permittivity occurs between the paraelectric and ferroelectric phases [149]. By accepting the idea of chemical inhomogeneity responsible for relaxor behaviour, Cross proposed a superparaelectric model, which believes that the polar clusters have different sizes and local symmetry (having local polarization vectors) is lower than global symmetry [39]. Further, the polar clusters exhibit two different states of polarization, *viz.,* +P and -P, and the dielectric relaxation occurs by switching between these states of polarization via thermal energy. The energy barrier between these thermally activated polarization fluctuations is low, and it depends on the size of the polar clusters. The frequency of fluctuation decreases by decreasing the temperature (lowering of thermal energy), leading to a dispersion in the dielectric permittivity peak. Finally, at low temperatures, the polarization vectors freezes along a specific direction. It was pointed out by Cross that analogous to superparamagnetism, the polarization present within the polar clusters in relaxor ferroelectrics varies as a function of temperature. Therefore, the freezing of polarization vectors can be expected on lowering the temperature (slowing of dielectric

relaxation) like the spin glass [39]. Consequently, Viehland proposed a dipolar glass model in order to include the interactions between the polar clusters in close analogy with the magnetic spin glasses [142, 150]. According to this model, the interaction between the polar clusters increases on lowering the temperature, and at sufficiently low temperatures, the dynamically disordered regions freezes, resulting into a frustrated polar state. The temperature-dependent variation in the dielectric permittivity was successfully modeled by the Vogel-Fulcher relationship [150], given below originally derived for the magnetic spin glass system.

$$f = f_0 exp\Big(-\frac{E_a}{k_B(T_m - T_{VF})}\Big) \tag{1.10}$$

where f is the frequency of measurements, f_0 is the pre-exponential factor (attempt frequency), k_B is the Boltzmann constant, E_a is the activation energy, and T_{VF} is called the Vogel–Fulcher freezing temperature. It has been observed that the ferroelectric and piezoelectric properties show a significant change with reference to the freezing temperature. Below the freezing temperatures, the dynamics of the PNRs gets significantly reduced, and a long-range ordered ferroelectric phase is stabilized on the application of an electric field. This ferroelectric phase remains stable until the system is subjected to a higher temperature above the freezing temperature. A relaxor ferroelectric material below T_{VF} is commonly referred to as the non-ergodic relaxor, whereas above T_{VF}, it is referred to as ergodic relaxor [135]. Further, it was argued by Viehland *et al.* that above the freezing temperature, fluctuations in polarization can be visualized as a consequence of polarization rotation between the equivalent orientations [142, 150]. Glazunov *et al.* proposed a breathing model to explain relaxors. In this model, the relaxor is considered as a system of randomly distributed PNRs, within the nonpolar matrix [151]. The boundaries of the PNRs are pinned due to internal random electric fields generated by charge disorder. Additionally, the model considers that the PNRs are stabilized in orientation along one of the directions compatible with the constraints of the polar phase, and the polarization

responses of the material in an ac field occur due to the vibration of the boundaries of PNRs [151]. Further, a 'random field model' model was proposed by Westphal, Kleemann, and Glinchuk to explain the relaxor ferroelectrics [152]. According to this model, the disordered distribution of the hetrovalent ions leads to quenched random electric fields, which breaks the formation of the long-range ordered ferroelectric state, resulting into small-size domains with definite polarization (analogous to PNRs). One of the successful achievements of random field theory was the explanation of relaxor ferroelectric behaviour of Ba(Sn,Ti)O_3 and Ba(Zr,Ti)O_3 with isovalent substitutions at 'B' site. This is in contrast to hetrovalently substituted systems (*e.g.,* Pb($Mg_{1/3}Nb_{2/3}$)O_3) where the charge disorder has been considered as an essential requirement for relaxor nature. The relaxor behaviour in these isovalently substituted cations has been predicted to be the consequence of the increase in the non-ferroelectric environment (e.g., paraelectric $BaSnO_3$ in ferroelectric $BaTiO_3$), which breaks the long-range ferroelectric ordering. Thus the isovalent substitution of Sn^{4+}/Zr^{4+} at Ti^{4+} site results into the distortion of [TiO_6] octahedra which in turn generates the ferroelastic domain state [152]. Therefore, the induced relaxor nature has been attributed to the random local strain field generated by the ferroelastic domain states [152]. Further, some of the studies utilize the balance between the short-range repulsions and bonding considerations to explain the relaxor behaviour present in the materials [9, 133]. In normal ferroelectrics, the ferroelectric distortions are determined by the balance between the short-range repulsions and dipole-dipole interactions. The balance between these forces is altered by the hybridization between the electronic states of cations (e.g., 3*d* state of Ti in $BaTiO_3$) and the 2p states of oxygen, which in turn affects the transition temperature [133]. If the material is completely ordered, then all the constituent ions are affected by similar forces. On the other hand, similar crystallographic sites are occupied by different cations in compositionally disordered materials. Thus, the interatomic interactions which cause the phase transition becomes random, and therefore

the long-range polar ordering gets disturbed [133]. Glinchuk and Farhi (GF) proposed an order-disorder model of the transition [153]. This model considers the high-temperature phase as the one consisting of reorientable dipoles in a highly polarizable matrix. The high polarizability of the matrix is linked with the presence of transverse optic soft phonon mode in the relaxors [133]. Therefore according to the soft mode theory, the FE phase should appear at low temperatures due to freezing of the soft phonon mode. Hence, in order to explain the absence of a macroscopic ferroelectric phase in the relaxors, additional local statics/dynamics (*i.e.,* the condensation of soft modes at local levels creating PNRs) have been considered, which is large enough to hamper the long-range ordered ferroelectric phase. Bokov *et al.* proposed that in the case of 'A' and 'B' site-modified perovskite-based relaxors, various kinds of random interactions exist, which makes the dipoles non-identical, and the PNRs are thought to be the result of local condensation of soft phonon modes. Further, based on the composition of the material, the degree of diffuseness can be predicted. The degree of diffuseness increases with an increase in the difference in the ionic radii of the dopants of ferroelectrically active sublattice corresponding to the 'A' or 'B' site of the perovskite structure [133]. In addition to these, various other models such as spherical random-bond–random-field model [154], bi-relaxation mode [135, 155], etc., have also been proposed to describe the underlying mechanism in the relaxor ferroelectric materials.

Our analysis reveals that the underlying key features responsible for high physical properties, *viz.,* morphotropic phase boundary and relaxor behaviour have been very much exploited for lead-based systems, and that is why they dominate in the market of ferroelectric materials. However, owing to its toxic and hazardous nature, various efforts are being made for the development of lead-free alternatives [31, 32, 33, 34]. Therefore, several lead-free solid solutions exhibiting the key features (such as polymorphic, morphotropic phase boundary, and relaxor behaviour) responsible for the high physical responses of the system have been fabricated. In this regard, $BaTiO_3$-based systems having partial

homovalent substitutions corresponding to 'A' or (and) 'B' sites such as (Ba,Ca)TiO_3, Ba(Zr,Ti)O_3, Ba(Sn,Ti)O_3, (Ba,Ca)(Zr,Ti)O_3, (Ba,Ca)(Sn,Ti)O_3, etc., have emerged as highly appealing technologically important candidates.

1.6 Literature review on some $BaTiO_3$-based lead-free functional materials

1.6.1 (Ba,Ca)TiO_3

The studies performed in the past have clearly demonstrated that lead-titanate ($PbTiO_3$) exhibits relatively larger ferroelectricity than barium titanate ($BaTiO_3$) [91]. Various studies have predicted that one of the reasons behind the high ferroelectricity lies in the larger value of lattice strain exhibited by $PbTiO_3$ ($\frac{c}{a}$ = 1.06) than $BaTiO_3$ ($\frac{c}{a}$ = 1.01) [16, 85]. Also, in perovskite-based materials, it has been reported that the larger value of lattice strain can modify the nature of the ferroelectric ground state, and the nature of phase transitions [16, 85]. Thus based on lattice strain values, the $PbTiO_3$ (PT) exhibits a ground state tetragonal phase, while barium titanate shows a ground state consistent with the constraints of rhombohedral symmetry [16]. Previous studies have linked the high lattice strain with the stable nature of the ferroelectric phase, and the enhancement in the ferroelectric polarization [16, 156, 157, 158]. Thus the control of tetragonality may be one of the efficient ways in order to enhance ferroelectric polarization. In this regard, the A(Ca^{2+}) site modified $BaTiO_3$-based solid solution, *i.e.,* ($Ba_{1-x}Ca_x$)TiO_3 (BCT), has been recognised to be highly promising because of the anomalous evolution of lattice strain (*i.e.,* nearly unchanged $\frac{c}{a}$ parameter) and nearly constant saturation polarization within the solid solubility limit [159]. The phase diagram of (Ba,Ca)TiO_3 (BCT) shows that the incorporation of Ca in $BaTiO_3$ nearly sustains the Curie temperature (T_c) while it lowers the T-O and O-R phase transitions (see Fig. 1.12 (a)) [7, 44, 160]. Thus BCT leads to a

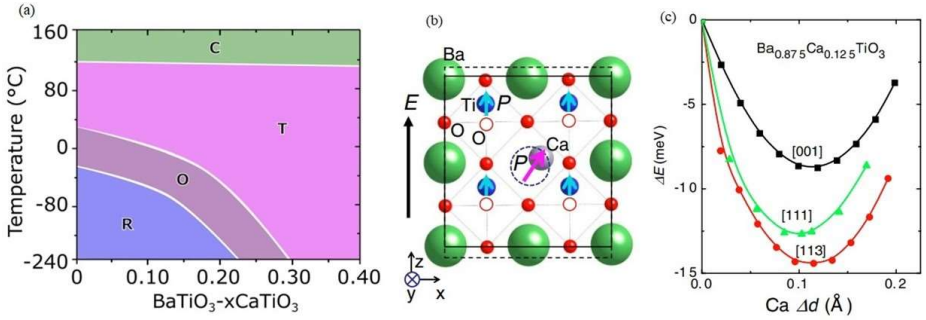

Fig. 1.12 (a) Phase diagram of $BaTiO_3$-$x$$CaTiO_3$ ceramics [6], (b) representation of off-centered calcium atoms in the tetragonal phase of $BaTiO_3$-$x$$CaTiO_3$ [7], and (c) the relative energies of $BaTiO_3$-$x$$CaTiO_3$; $x = 0.125$ for off-centered Ca atoms along [001], [111], and [113] directions [7].

tetragonal (*P*4*mm*) phase spanning over a wide temperature range, which becomes stable down to 0 K for the compositions having large Ca content [7, 44]. The analysis performed by different groups on BCT observed a high ferroelectric polarization, large dielectric permittivity with low loss, and high piezoelectric coefficient [7, 44]. These properties have been linked with the similar role of Ca^{2+} cations corresponding to the 'A' site of BCT as Pb^{2+} does in lead-titanate [7, 49]. Fu *et al.* observed that, even though the Ca-O bond is ionic in BCT, in contrast to the covalent Pb-O bond in lead titanate, the Ca^{2+} cations become locally off-centered because they have a smaller ionic radius than Ba^{2+} cations (see Fig. 1.12 (b)) [7]. Further, based on first principles calculations for $(Ba_{0.875}Ca_{0.125})TiO_3$, Fu *et al.* found that the off-centered Ca^{2+} cations locate along [113] directions which neither corresponds to the constraints of tetragonal or rhombohedral symmetry (see Fig. 1.12 (c)) [7]. However, the four equivalent directions along which Ca^{2+} cations become off-centered are [113], [$1\bar{1}3$], [$\bar{1}13$], [$\bar{1}\,\bar{1}3$], and the tetragonal phase corresponding to this composition, *i.e.,* Ca(x) = 0.125, was believed to be associated with the thermal and spatial averaging between these states. In addition, the ferroelectrically active Ca^{2+} cations also promote the off-centering of Ti^{4+} cations corresponding to 'B' sites, as Pb^{2+} does in $PbTiO_3$, and, consequently leads to significant enhancement in ferroelectric polarization

[7]. Later Levin *et al.* also reported a similar analogy between (Ba,Ca)TiO_3 and $PbTiO_3$ [49].

1.6.2 Ba(Sn,Ti)O_3

In the discovery of 'B' site substituted $BaTiO_3$-based ceramics, the Sn-doped $BaTiO_3$, *i.e.,* Ba(Sn_yTi_{1-y})O_3 (BST), has been found to exhibit significantly enhanced dielectric, ferroelectric, and piezoelectric properties [8, 161]. Ba(Sn,Ti)O_3 (BST) ceramics are fabricated by forming the solid solution of ferroelectric barium titanate ($BaTiO_3$) with paraelectric barium stannate ($BaSnO_3$) [2, 8, 162]. In BST ceramics, the physical properties are found to be adjustable by tuning the ratio of Sn/Ti content, and consequently developing the phase coexistence region resulting into modifications in microstructural characteristics such as grain size, grain boundaries, etc. [8, 163]. The solid solutions of BST ceramics have proven itself to be very important for the electroceramic industry because of its exotic physical responses. It finds wide application in voltage-controlled oscillators, variable capacitors, microwave dielectric amplifiers, phase shifters, tunable filters, etc. [9, 164]. In view of the crystallographic structural phase transitions, the increase in Sn content in Ba(Sn,Ti)O_3 increases T-O and O-R phase transitions whereas lowers the C-T phase transition temperature, thereby making them coalesce slightly above room temperature around Sn(y) = 0.11 (see Fig. 1.13) [8]. However, various studies differ regarding the exact crystallographic phase(s) corresponding to the particular compositions. In this regard, studies performed by Horchidan *et al.* via structural, dielectric, and ferroelectric analysis of Ba(Sn_yTi_{1-y})O_3 for ($0 \leq$ Sn(y) ≤ 0.20) system demonstrates a single $P4mm$ phase for Sn(y) = 0, a mixture of $Amm2$ and $P4mm$ phases for Sn(y) = 0.05, a single $P4mm$ phase for Sn(y) = 0.10, $P4mm$+ $Pm\bar{3}m$ phase for Sn(y) = 0.15, and finally, a cubic $Pm\bar{3}m$ phase for Sn(y) = 0.20. For the composition with Sn(y) = 0.05, the highest ferroelectric polarization was observed, linked with the appearance of the orthorhombic phase at this composition.

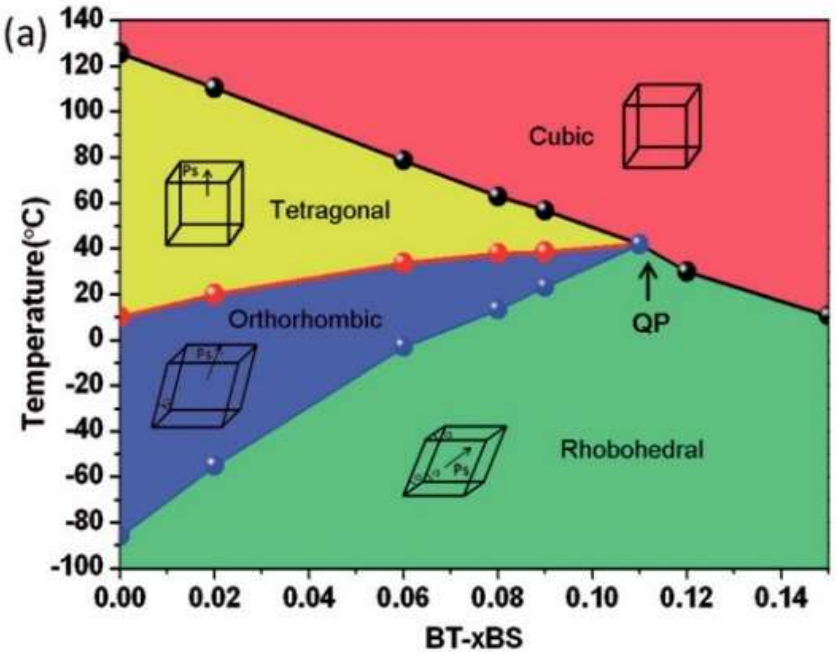

Fig. 1.13 Phase diagram of Ba(Sn,Ti)O_3 as a function of Sn content [8].

Further, for Sn(y) = 0.15, a high value of room temperature dielectric constant $\sim$ 12500 was reported due to the proximity of paraelectric-ferroelectric phase transition near the room temperature [163]. On the other hand, Veselinovic *et al.* carried out the structural investigations via X-ray diffraction, Raman spectroscopic analysis, transmission electron microscopy (TEM), high-resolution TEM (HRTEM), and selected-area electron diffraction (SAED), for composition range ($0 \leq$ Sn(y) ≤ 0.20). The Rietveld refinements revealed the presence of a $P4mm$ phase for $0 \leq$ Sn(y) ≤ 0.07, a coexisting $P4mm$+$Pm\bar{3}m$ phase for Sn(y) = 0.10, and a single $Pm\bar{3}m$ phase for higher compositions [165]. Moreover, short-range structural investigations carried out via Raman spectroscopic analysis have shown a tetragonal ($P4mm$), and a small fraction of orthorhombic ($Pmm2$) phases throughout the analysed compositions [165]. Whereas according to Deluca *et al.*, the transformation from $P4mm$ ($0 \leq$ Sn(y) ≤ 0.10) to the $P4mm$+$Pm\bar{3}m$ phase occurs at Sn(y) = 0.15, which thereafter shows a single cubic phase for Sn(y) = 0.20 [164]. In addition, a long-range ordered normal ferroelectric to a short-range ordered relaxor ferroelectric phase transition

was observed for Sn(y) = 0.20 [164]. The phase diagram of BST ($0 \leq$ Sn(y) ≤ 0.20) was re-investigated by Veselinovic *et al.* via performing the neutron diffraction analysis and reported a transformation from *P*4*mm* (Sn(y) = 0) to a coexisting *P*4*mm*+*Amm*2 phase over $0.025 \leq$ Sn(y) ≤ 0.07, which transforms into another two-phase (*R*3*m*+*Pm*$\bar{3}$*m*) coexistence region stable for $0.10 \leq$ Sn(y) ≤ 0.12, and thereafter, a single cubic phase for Sn(y) = 0.15 and 0.20 [166]. Yao *et al.* observed a quasi-quadruple point (nearly the coexistence of C-T-O-R phases) around Sn(y) = 0.11, slightly above room temperature, and reported a huge piezoelectric coefficient (d_{33} = 697 pC/N) along with a very high dielectric constant [8]. The origin behind this high piezoresponse has been argued to be the minimized energy barriers, facilitating the easy polarization rotation and extension phenomenon demonstrated via the Landau-Devonshire model [8]. However, the existence of a quadruple point in binary solid solution immediately raised the question regarding its compatibility with the Gibbs phase rule. Later, using Landau's theory, Ke *et al.* suggested that at the quasi quadruple point, two first-order phase transition lines corresponding to T-O and O-R phases and two second-order transition lines corresponding to C-T and C-R phases meet without defying the thermodynamic phase rule on composition *vs.* temperature phase diagram [167]. Extending the structure-property correlation studies in $Ba(Sn_yTi_{1-y})O_3$, Kalyani *et al.* analysed the compositions over the range ($0 \leq$ Sn(y) ≤ 0.12) by subjecting them to both X-ray and neutron diffraction analysis assisted via dielectric and ferroelectric measurements and observed that the system posses a coexisting *P*4*mm*+*Amm*2 phase for ($0.02 \leq$ Sn(y) ≤ 0.08), and thereafter a single rhombohedral phase till ($0.10 \leq$ Sn(y) $\leq$ 0.12). Further, Kalyani *et al.* observed that the system exhibits an anomalous piezoelectric response for the dilute Sn concentration; ($0.02 \leq$ Sn(y) ≤ 0.04). This high piezoresponse was argued to be an effect of the propensity of polarization switching from [100] to [101] pseudocubic direction as a function of the electric field, which enhances significantly by tuning T-O phase transition in the vicinity of room temperature [161]. Furthermore, Ren *et*

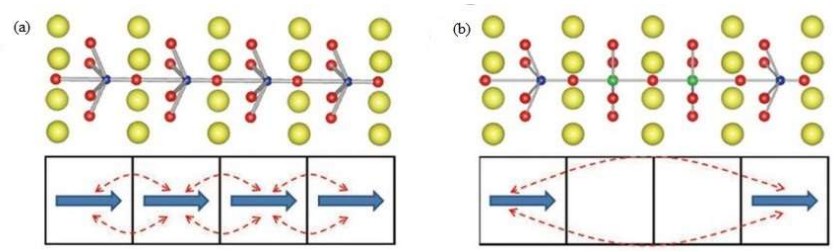

Fig. 1.14 (a) The dipole-dipole interaction in $BaTiO_3$ (b) and the interaction between the dipoles in $Ba(Sn_{0.20}Ti_{0.80})O_3$; The blue and green colours represent the Ti and Sn atoms [9].

al. observed a single tetragonal phase for Sn(y)$\leq$0.04, a rhombohedral phase for Sn(y) = 0.11, and finally, a cubic phase for ($0.15 \leq$ Sn(y) ≤ 0.30). Moreover, Ren *et al.* identified Sn(y) = 0.15 as a composition having an intermediate state between the normal and relaxor ferroelectrics giving rise to high dielectric tunability, driven by the co-contribution from the domain, domain wall motion, and polar clusters [168]. In addition to these, many studies completely devoted to explore the relaxor ferroelectricity in $Ba(Sn,Ti)O_3$ have also been a subject of research for various groups. Around Sn(y) = 0.15, the presence of a diffuse phase transition has been identified in numerous studies [169, 170]. The analysis performed by different groups demonstrates the existence of ferroelectric-like regions above the Curie temperature. As per the report of Xei *et al.*, both the dynamic and static PNRs exist above the Curie temperature, which finally transforms into a ferroelectric phase when the temperature is lowered below the Curie temperature [170]. Shravatsman *et al.* reported the presence of a mixed ferroelectric and relaxor state for $0.175 \leq$ Sn(y) ≤ 0.25 and a typical relaxor ferroelectric state for Sn(y) = 0.30 [171]. Various other groups have also thrown light on relaxor behaviour in BST ceramics [9, 47, 48, 163, 169, 172, 173, 174]. Shi *et al.* suggested that in normal ferroelectrics such as $BaTiO_3$, every unit cell possesses the dipoles generated due to off-centered Ti^{4+} cations, and their interaction leads to a long-range coulomb field (see Fig. 1.14). These dipoles appear due to a covalent character of Ti-O bonds, which is governed by a strong hybridization between the 3d electronic

states of the Ti^{4+} cations and the $2p$ states of O^{2-} anions. Further, Shi *et al.* demonstrated that the orbital hybridization between Sn and O atoms becomes much weaker than the one present between Ti and O atoms [9]. Therefore, the dipole can barely occur in the unit cells where Ti atoms have been replaced by Sn, and thus the dipole-dipole interaction existing over a long-range gets disrupted, explaining the origin of relaxor behaviour in the $Ba(Sn_yTi_{1-y})O_3$ ceramics (see Fig. 1.14) [9].

1.6.3 Ba(Zr,Ti)O_3

Barium zirconate titanate, *i.e.,* $Ba(Zr_zTi_{1-z})O_3$ (BZT) is the solid solution of ferroelectric barium titanate ($BaTiO_3$) with incipient ferroelectric barium zirconate ($BaZrO_3$) [2, 175, 176]. The term incipient ferroelectric refers to the systems that possess an unstable phonon mode corresponding to the Γ point of the cubic Brillouin zone (responsible for ferroelectric behaviour of materials), but the amplitudes of quantum zero-point motion dominates over ferroelectric distortions, which in turn prevents the establishment of long-range ferroelectric ordering [177, 178]. However, its solid solution with ferroelectric $BaTiO_3$ leads to a very interesting phase diagram which consequently gives rise to fascinating physical responses useful for various technological applications such as transducers, multilayer capacitors, infrared detectors, and tunable devices for microwave electronics [179]. The phase diagram of BZT comprises many inter-ferroelectric phase transitions that appeared at the macroscopic level, as well as several structural modifications at the microscopic level, with the increase in Zr content. The increase of Zr content decreases the paraelectric to ferroelectric phase transition temperature and increases the inter-ferroelectric phase transition temperatures, and a pinched phase transition occurs where all the three phase transitions corresponding to pure $BaTiO_3$ merge at a point in composition *vs.* temperature phase diagram (see Fig. 1.15) [46, 180]. Further, for Zr(z) = 0.25, BZT transforms into a relaxor ferroelectric state which remains stable till Zr(z) = 0.75; after that, it behaves

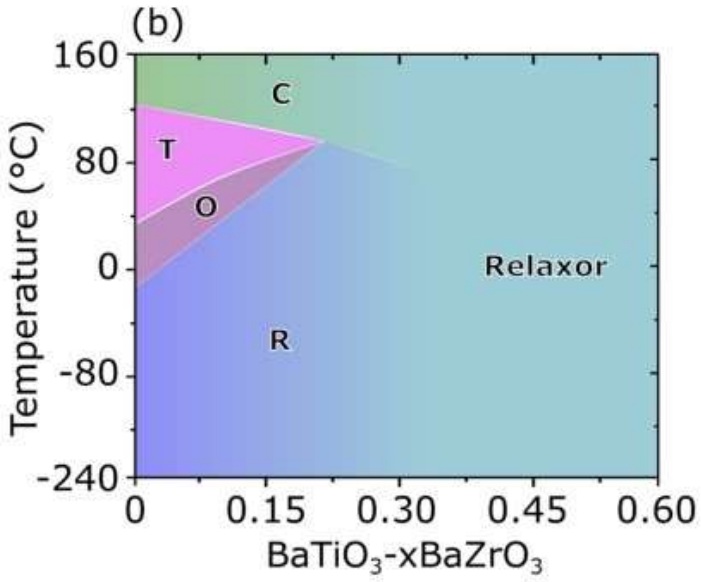

Fig. 1.15 Phase diagram of $BaTiO_3$-$BaZrO_3$ [6].

like a dipolar glass up to Zr(z) = 0.95, and finally transforms into quantum paraelectric $BaZrO_3$ [46, 176]. Here, it is worth notable that various studies have been performed regarding the structure-property correlations in BZT for both the conventional ferroelectric as well as relaxor ferroelectric regime. The structural investigations carried out by Kalyani *et al.* over the conventional ferroelectric compositions via Rietveld refinements of the powder diffraction data have revealed a coexistence of *P*4*mm* and *Amm*2 phase stable for $0.02 \leq \text{Zr}(z) \leq 0.05$, coexisting *Amm*2 and *R*3*m* phases stable for $0.07 \leq \text{Zr}(z) < 0.09$, and a single *R*3*m* phase stable up to $0.09 \leq \text{Zr}(z) \leq 0.16$ [181]. Recently, Peng *et al.* reported a T-O phase boundary at Zr(z) = 0.013, O-R phase boundary at Zr(z) = 0.0798, and C-R phase boundary at Zr(z) = 0.2135, using thermodynamic potential approach [180]. In addition to these global structure determinations, various efforts have been made in BZT to predict the structure at the microscopic level since it is very well established that one of its end members, *i.e.*, $BaTiO_3$, consists of a local rhombohedral symmetry [88, 107, 182, 183]. The Raman spectroscopic studies independently performed by Farahi *et al.* and Karan *et al.* revealed rhombohedral-like polar nano-regions for BZT relaxors

[184, 185]. EXAFS studies performed by Laulhe *et al.* predicted the segregation of Zr atoms at the local scale to form $BaZrO_3$-like clusters in the $BaTiO_3$-like matrix [186]. Using density functional theory and X-ray absorption fine structure (XAFS) studies, Levin *et al.* predicted that the isolated Ti atom present within the large octahedral site of $BaZrO_3$ occupies the centrosymmetric position; however, when adjacent $BaTiO_3$ unit cells occur, a polar off-centering of Ti is observed [187]. The neutron pair distribution function analysis performed by Laulhe *et al.* for some relaxor compositions has shown that the nature of $[ZrO_6]$ and $[TiO_6]$ is similar to that of $BaZrO_3$ and $BaTiO_3$, which means the Zr ion remains at the center of the octahedra, whereas Ti exhibits a local off-centering along <111> directions [188]. Buscaglia *et al.* also observed a similar local off-centering of Ti^{4+} cations along <111> directions for compositions Zr(z) = 0.10, 0.20, and 0.40, based on PDF data obtained by total X-ray scattering experiments [189]. Pramanic *et al.* also observed the presence of local disorder along <111> directions in BZT, corresponding to 'B' sites [190]. However, overwhelming research on BZT has been carried out in its relaxor ferroelectric region. Maiti *et al.* observed that the relaxor ferroelectric region in BZT is stable for $0.25 \leq \text{Zr}(z) \leq 0.70$ and can be divided into two categories, one of which comprises the lower Zr content $0.25 \leq \text{Zr}(z) \leq 0.45$, where T_m decreases as Zr content increases, while other for $0.45 < \text{Zr}(z) \leq 0.70$, where T_m remains nearly constant as a function of Zr content [148]. The relaxor behaviour in BZT has been described by the difference in ionic radii of the Zr^{4+} and Ti^{4+} cations corresponding to the 'B' sites. This difference induces a shear strain which results into elastic interaction between the nonpolar and polar regions governed by Zr^{4+} and Ti^{4+} cations. Further, as $BaZrO_3$ has a greater volume than $BaTiO_3$, the nearby Zr-centered octahedra will exert a compressive strain, likely a shear strain, on the Ti-centered octahedra. This strain-induced displacement of Ti^{4+}-O^{2-} results in local dipoles with non-vanishing polarisation [148, 176, 191, 192]. These displacements, which are caused by the local strains induced by the two distinct types of octahedra, will generate

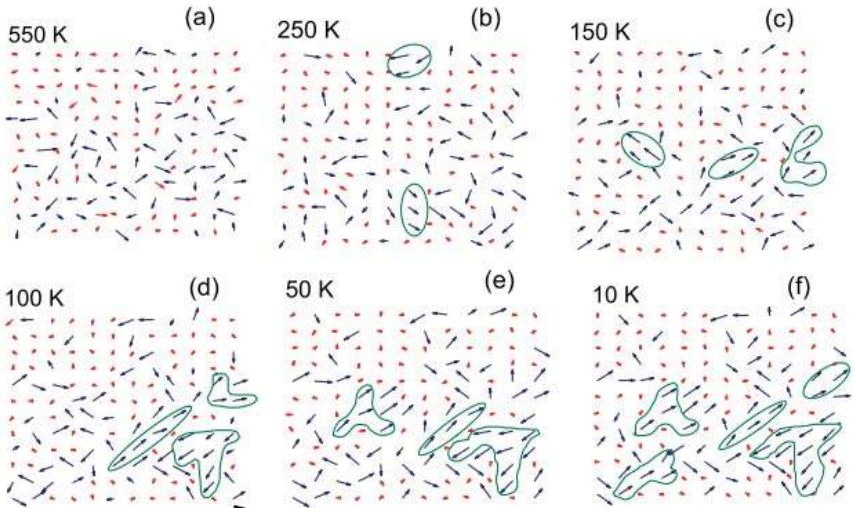

Fig. 1.16 Temperature-dependent evolution of polar nano-regions in relaxor ferroelectric state of (Ba,Zr)TiO_3. Blue colour and red colours correspond to the Ti and Zr ions [10].

random fields, which in turn modifies the dipole moments corresponding to Ti-O bonds. Moreover, the elastic interactions acting between the nonpolar and polar regions do not remain long-range type for the compositions above 25 mol % of $BaTiO_3$, and beyond this content of $BaTiO_3$, polar clusters attain a critical size and density where BZT starts exhibiting the relaxor behaviour [135, 148, 176, 191, 192]. The temperature-dependent evolution of the polar clusters in BZT has been recently reported by Akbarzadeh *et al.* [10]. He has analysed the BZT system having equal concentrations of Zr and Ti atoms, allowing for the displacements of all the ions (a finite-size simulation) [10]. He found that at very high temperatures (T = 550 K), randomly oriented dipoles exist, which correspond to the Ti^{4+} cations, and these dipoles are surrounded by the small dipoles corresponding to Zr^{4+} cations (see Fig. 1.16) [10]. When the temperature is lowered (T = 250 K), some of the Ti sites act as a center around which the clusters start evolving, with the dipoles aligning parallel to each other [10]. However, at this stage, the orientation of the polarization was not lying along the <111> direction, but the average directions of the local polarization was found to lie along orthorhombic and triclinic directions. On further lowering of temperature

(T = 150 K), more clusters appear, making the average magnitude of Ti^{4+} dipoles even higher [10]. Also, some of the polar clusters start aligning along <111> direction. With the further lowering of temperature below 100 K, the clusters grow in size considerably with the polarization directed close to one of eight rhombohedral <111> directions, and some of the clusters get frozen (see Fig. 1.16) [10].

1.6.4 (Ba,Ca)(Zr,Ti)O_3

A remarkable breakthrough in the discovery of lead-free ceramics was achieved by the development of $BaTiO_3$-based system viz., $Ba(Zr_{0.20}Ti_{0.80})O_3$-$x(Ba_{0.70}Ca_{0.30})TiO_3$ (BZT-xBCT) system (first fabricated by Liu *et al.*), which exhibits significantly high piezoelectric properties (d_{33} = 620 pC/N), at MPB (x = 0.50), comprising of *P*4*mm*, and *R*3*m* phases (see Fig. 1.17) [11]. This high piezoelectricity was attributed to the presence

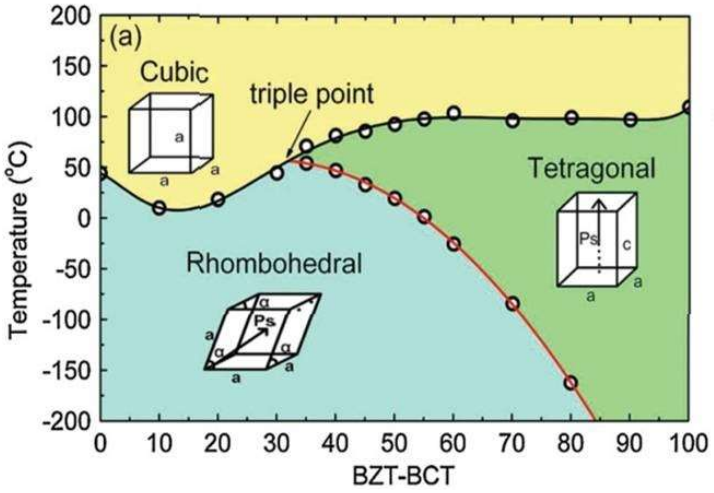

Fig. 1.17 Phase diagram of BZT-xBCT ceramics [11].

of a tricritical triple point lying in the proximity of MPB, leading to a very low energy barrier between the cubic, tetragonal, and rhombohedral phases, facilitating easy polarization rotation phenomenon [11]. However, the phase diagram proposed by Liu and Ren doesn't show any signature of the orthorhombic (*Amm*2) phase, whose possibility

could not be ruled out because of the presence of the *Amm*2 phase over a wide temperature range in the phase diagram of the host $BaTiO_3$. In this regard, numerous studies have been performed on BZT-*x*BCT ceramics via various techniques, *viz.,* powder diffraction analysis [193, 194], Raman spectroscopic studies [42], and microstructural analysis [195, 196, 197, 198], but the structure near MPB still remain a moot point. Using the convergent beam electron diffraction (CBED) technique, Gao *et al.* reported a T-R phase coexistence akin to one recently demonstrated by Ji *et al.* using Raman spectroscopic technique [195, 199]. This is similar to what was first ever reported by Liu *et al.* [11]. However, some recent investigations have pointed out the existence of an intermediate O phase sandwiched between the T and R phases, revealing the presence of two-phase boundaries, *viz.,* T-O and O-R (see Fig. 1.18), out of which the highest piezoresponse was reported for T-O phase boundary [42, 200]. Using Landau free energy calculations, Yang *et al.* attributed the high piezoresponse to T-O phase boundary with the lowest energy barrier between the T and O phases [12]. Keeble *et al.* observed that the O-R phase transition coalesces with the previously reported tricritical point by Liu and Ren, resulting into a phase convergence region [200]. Akbarzadeh *et al.* observed the orthorhombic (*Amm*2) phase as the ground state in BZT-*x*BCT for $0.83 \leq x \leq 0.86$ [201]. He argued that the orthorhombic ($|P_x| = |P_y| \neq 0$, $|P_z| = 0$) phase results due to suppression of one of the polarization components of the rhombohedral ($|P_x| = |P_y| = |P_z| \neq 0$) phase by quantum fluctuations [201]. Further structural studies extended by Brajesh *et al.* demonstrated a three-phase (T+O+R)

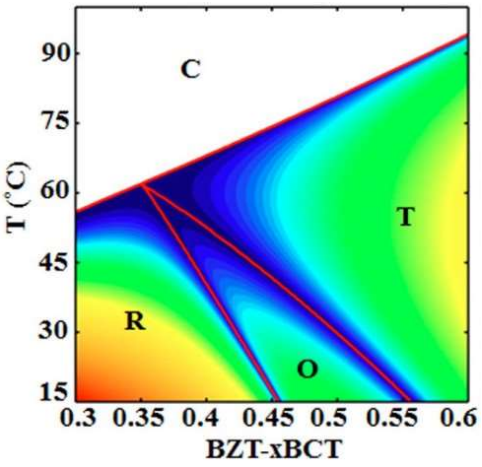

Fig. 1.18 Revised phase diagram of BZT-*x*BCT ceramics [12].

coexistence for $(Ba_{0.85}Ca_{0.15})(Zr_{0.10}Ti_{0.90})O_3$ and argued that the high electromechanical response for this composition results due to strong electric field dependency of the coexisting (T+O+R) phases [193]. Analysing Rietveld refinement of the powder diffraction data, Brajesh *et al.* revealed that on the application of the electric field, the tetragonal phase shows a higher propensity of transformation to the rhombohedral phase in comparison to the orthorhombic phase [193]. Further, he also observed a significant contribution in electromechanical responses from the presence of a weak dielectric relaxational behaviour [193]. The relaxor behaviour in $(Ba_{0.85}Ca_{0.15})(Zr_{0.10}Ti_{0.90})O_3$ ceramics appears due to the existence of random fields like the lead-based relaxors. However, the nature of the random field in $(Ba_{0.85}Ca_{0.15})(Zr_{0.10}Ti_{0.90})O_3$ was found to be different than the one observed in hetrovalent substituted lead-based relaxors such as $Pb(Mg_{1/3}Nb_{2/3})O_3$ (PMN). In PMN, the relaxor behaviour is driven by random electric fields generated due to charge disorder. However, in $(Ba_{0.85}Ca_{0.15})(Zr_{0.10}Ti_{0.90})O_3$, the cations corresponding to both the 'A' and 'B' sites of the perovskite structure are homovalent in nature, and thus, there can be no charge disorder. It is believed that the disordered distribution of Zr^{4+} and Ti^{4+} cations generate random stress due to a significant difference in the ionic radii of these cations, which consequently leads to a random stress field resulting in the relaxor behaviour [193].

1.6.5 (Ba,Ca)(Sn,Ti)O_3

The solid solution $(Ba,Ca)(Sn,Ti)O_3$ has got considerable attention in recent years because of interestingly high piezoelectric properties. Li *et al.* analysed the solid solutions $(Ba_{1-x}Ca_x)(Sn_{0.04}Ti_{0.96})O_3$ and $(Ba_{1-x}Ca_x)(Sn_{0.06}Ti_{0.94})O_3$ for $(0 \leq Ca(x) \leq 0.04)$, and reported the high piezoelectric coefficient d_{33} = 440 pC/N and d_{33} = 510 pC/N for $(Ba_{0.97}Ca_{0.03})(Sn_{0.04}Ti_{0.96})O_3$ and $(Ba_{0.98}Ca_{0.02})(Sn_{0.06}Ti_{0.94})O_3$ respectively [43, 45]. This high piezoelectric response was attributed to the tetragonal-orthorhombic phase coexistence [43, 45]. Similarly, Zhu *et al.* investigated $(Ba_{1-x}Ca_x)(Sn_{0.08}Ti_{0.92})O_3$ $(0 \leq Ca(x)$

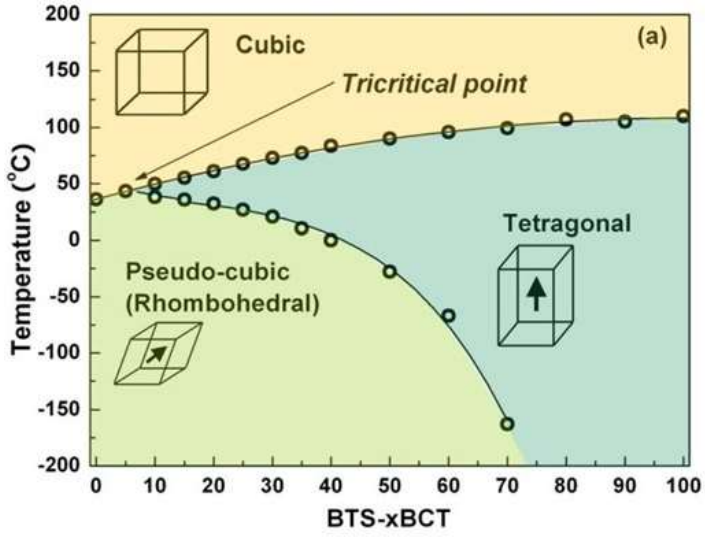

Fig. 1.19 Phase diagram of $Ba(Sn_{0.12}Ti_{0.88})O_3$- $x(Ba_{0.70}Ca_{0.30})TiO_3$ ceramics [13].

≤ 0.06) and observed d_{33} = 568 pC/N and k_p = 47.7%, along with high dielectric constant at Ca(x) = 0.05, which exhibits a phase coexistence of tetragonal and orthorhombic phases [202]. Similarly, Chen *et al.* investigated $(Ba_{1-x}Ca_x)(Sn_{0.05}Ti_{0.95})O_3$ ($0 \leq$ Ca(x) $\leq$ 0.07), and observed high piezoelectric coefficient (d_{33} = 464 pC/N) and electromechanical coupling factor (k_p = 43.1%) at Ca(x) = 0.02, having a tetragonal-orthorhombic phase coexistence [203]. Zhu *et al.* investigated $BaTiO_3$-$x(CaTiO_3$-$BaSnO_3)$ and obtained a high piezoelectric coefficient (d_{33} = 570 pC/N), low coercive field, and high ferroelectric polarization for x = 0.16 as a consequence of multi-phase (T+O+R) coexistence which leads to low energy barrier between the phases facilitating easy polarization [204]. Further, the analysis performed by Zhu *et al.* on $(Ba_{0.90}Ca_{0.10})TiO_3$-$xBa(Sn_{0.20}Ti_{0.80})O_3$ revealed a multi-phase (T+O+R) for x = 0.45, due to an extremely low energy barrier between the three phases, leading to easy polarization rotation phenomenon, which in turn results in extremely high piezoelectric coefficient (d_{33} = 630 pC/N) [205]. In addition, Xue *et al.* reported high piezoelectric coefficient (d_{33} = 530 pC/N), corresponding to the composition x = 0.30 in $Ba(Sn_{0.12}Ti_{0.88})O_3$- $x(Ba_{0.70}Ca_{0.30})TiO_3$ (see Fig. 1.19) [13]. This high response was attributed to the appearance of tetragonal-rhombohedral phase boundary

corresponding to this composition [13]. Further, Zhu *et al.* performed the X-ray diffraction, dielectric, and piezoelectric studies on $(Ba_{0.95}Ca_{0.05})(Sn_xTi_{1-x})O_3$ and observed the high piezoelectric coefficient (d_{33} = 670 pC/N) around Sn(x) = 0.11 and linked this with the multi-phase (rhombohedral, pseudocubic and orthorhombic) coexistence [206]. Recently, Kim *et al.* reported a high d_{33} = 480 pC/N along with high ferroelectric polarization in $Ba(Sn_{0.20}Ti_{0.80})O_3$-$x(Ba_{0.90}Ca_{0.10})TiO_3$ corresponding to the composition x = 0.55 and considered this to be due to MPB like tetragonal-orthorhombic phase coexistence [207]. Abebe *et al.* performed a comparative study of piezoelectric properties in (Ba,Ca)(Sn,Ti)O_3 and Ba(Sn,Ti)O_3 and found that large piezoelectric coefficient of (Ba,Ca)(Sn,Ti)O_3 ceramics is driven by the unique combination of improved polarization (associated with the enhancement in the covalent character of the Ti-O bond caused by the Ca substitution) and domain wall motion (enabled via reduced lattice strain) [208].

1.7 Organisation of the thesis

The remainder of this thesis has been organised as follows:

The chapter 2 describes the details of the sample synthesis and the characterization techniques.

The chapter 3 describes the significant role of calcium dopant at the 'A' site in tuning the ferroelectric polarization and the dielectric relaxor behaviour in the centrosymmetric cubic ($Pm\bar{3}m$) phase of the so-developed smart material $(Ba_{1-x}Ca_x)(Sn_{0.11}Zr_{0.05}Ti_{0.84})O_3$; BCSZT$x$ ($0 \leq x \leq 0.20$).

The chapter 4 is based on the temperature-dependent crystallographic phase transitions of the relaxor ferroelectric $(Ba_{0.85}Ca_{0.15})(Sn_{0.11}Zr_{0.05}Ti_{0.84})O_3$ system.

In chapter 5, we discuss the role of Γ_4^- (k=0,0,0) soft phonon mode corresponding to the cubic ($Pm\bar{3}m$) phase in tuning various ferroelectric phase transitions and

its impact on dielectric and ferroelectric properties of the lead-free functional material $(Ba_{0.92}Ca_{0.08})(Zr_{0.05}Ti_{0.95\text{-}x}Sn_x)O_3$; BCZTSn$x$ $(0 \leq x \leq 0.10)$.

Further, chapter 6 describes the role of 'Sn' in tuning the dielectric relaxor behaviour and short-range ordering for BCZTSnx $(0.125 \leq x \leq 0.25)$ ceramics within the cubic phase field.

Finally, chapter 7 presents the summary of the thesis work and its future scope.